MRS Communications (2018), *8*, 398–403

doi:10.1557/mrc.2018.60

MRS Communications

Research Letter

Synthesis of fluorescent $CuInS_2$/ZnS quantum dots—porphyrin conjugates for photodynamic therapy

Ncediwe Tsolekile, Department of Applied Chemistry, University of Johannesburg, P. O. Box 17011, Doornfontein 2028, Johannesburg, South Africa; Centre for Nanomaterials Science Research, University of Johannesburg, Johannesburg, South Africa; Department of Chemistry, Cape Peninsula University of Technology, P.O. Box 652, Cape Town 2000, South Africa
Vuyelwa Ncapayi, Sundararajan Parani, and **El Hadji Mamour Sakho,** Department of Applied Chemistry, University of Johannesburg, P. O. Box 17011, Doornfontein 2028, Johannesburg, South Africa; Centre for Nanomaterials Science Research, University of Johannesburg, Johannesburg, South Africa
Mangaka C. Matoetoe, Department of Chemistry, Cape Peninsula University of Technology, P.O. Box 652, Cape Town 2000, South Africa
Sandile P. Songca, Department of Chemistry, University of Zululand, PB X1001, Kwadlangezwa 3886, South Africa
Oluwatobi S. Oluwafemi, Department of Applied Chemistry, University of Johannesburg, P. O. Box 17011, Doornfontein 2028, Johannesburg, South Africa; Centre for Nanomaterials Science Research, University of Johannesburg, Johannesburg, South Africa

Address all correspondence to Oluwatobi S. Oluwafemi at **ooluwatobi@uj.ac.za**, **Oluwafemi.oluwatobi@gmail.com**

(Received 24 January 2018; accepted 2 April 2018)

Abstract

Porphyrins are photosensitisers used in photodynamic therapy (PDT) due to their tumor localization and in situ singlet oxygen generation. However, their limited absorption, insolubility, and aggregation in an aqueous medium limited their effective application in PDT. To overcome these limitations, we herein, report a large-scale aqueous synthesis of $CuInS_2$/ZnS ternary quantum dots, and its conjugation to 5, 10, 15, 20-meso(4-hydroxyphenyl) porphyrin. The singlet oxygen generation of this highly aqueous soluble novel conjugate shows its potential for PDT applications.

Introduction

Photodynamic therapy (PDT) is a therapeutic process that has progressively developed for the treatment of several types of cancers, infections, and inflammatory conditions. As an alternative to chemotherapy, surgery, and other treatment modalities, PDT is less invasive, cheaper, tumor-specific, and can be easily administered to outpatients.[1, 2] Successful PDT is achieved via two types of mechanisms initiated by the irradiation of a photosensitizer (PS) with the light of specific wavelength to generate singlet oxygen species. Type 1 mechanism occurs when PS-drug at excited state reacts with organic substrates and produces free radical or radical ions which then react with biomolecules or oxygen to produce reactive oxygen species. Type 2 involves energy transfer from the activated PSs to oxygen molecules ($^3O_2$) in the excited singlet state to generate singlet oxygen ($^1O_2$) responsible for cell death.[3, 4] Several photosensitizing drugs have been reported which includes porfimer sodium (Photofrin), aminolevulinic acid (ALA/Levulan), Termofin (Foscan) with many new PSs currently being synthesized, namely the chlorins and bacteriochlorins.[5–7] Among these PSs, porphyrin-based PSs are the most commonly used due to their ability to localize in the tumor, low dark toxicity, and their ability to generate reactive singlet oxygen when irradiated with light of specific wavelength.[8, 9] Nonetheless, the insolubility of porphyrins in aqueous media and their inability to absorb in the near infrared (NIR) region (which is required for the treatment of deep-seated tumors) limits their use in PDT. One way of addressing these problems is through conjugation of porphyrins to nanomaterials such as quantum dots (QDs). There have been several reports on the conjugation of porphyrins to binary semiconductor nanocrystals from group II–VI (e.g., CdSe, ZnS, etc.) and group IV–VI elements (e.g., PbTe, PbS).[10–12] However, aggregation of these QDs–porphyrin conjugates and the inherent toxicity of the binary QDs attributed to the slow release of Cd^{2+} or Pb^{2+} ion into the surroundings[13, 14] have hindered their biologic applications. These limitations have given rise to an interest in ternary QDs such as $CuInS_2$ (CIS) QDs. Ternary QDs, possess unique optical and electronic properties such as tunable band gap to NIR region necessary for the therapeutic application, large Stokes shift, long fluorescence lifetime, and in addition, they have very low or non-bio toxicity.[15–17] Thus, they have been extensively investigated for biomedical, bio-imaging, in vivo, and in vitro applications.[16] As part of contributing toward effective use of porphyrin PS in PDT by overcoming the limitations mentioned above, we herein report the aqueous synthesis of ternary CIS/ZnS core/shell QDs and 5, 10, 15, 20-meso(4-hydroxyphenyl) porphyrin (mTHPP)—a "generation bridge" between the second and third generation of PSs in PDT. The as-prepared mTHPP was conjugated to the QDs, followed by singlet oxygen evaluation of both the porphyrin and the conjugate to determine its efficiency for PDT applications. As far as the authors know, there has never

been any report on the conjugation of this porphyrin to CIS QDs and its singlet oxygen evaluation. The as-synthesized conjugate was highly soluble in water without any aggregation even after 6 months. In addition, the conjugate exhibited high singlet oxygen quantum yield (0.72) compared with the pristine porphyrin (0.25), indicating the efficiency of the conjugate for PDT applications.

Experimental

Materials

Copper chloride, indium chloride, sodium citrate, L-glutathione, sodium sulfide, zinc acetate, thiourea, 4-hydroxybenzaldehyde, propionic acid, pyrrole, sodium bicarbonate ethanol, dichloromethane, methanol, ethyl acetate, *n*-hexane, chloroform, acetone, methylene blue, 3-diphenylbenzofuran, and dimethyl sulfoxide were purchased from Sigma Aldrich. All chemicals were of analytical grade and used without any purification except pyrrole which is distilled prior to use. Deionized water was used for all aqueous solution preparations.

Synthesis of CIS/ZnS QDs

The synthesis was carried out according to Chen et al.[18] method with modifications. Briefly, the synthesis of CIS core QDs with a Cu/In ratio of 1:4 was carried out hydrothermally in 2 L pressure cooker. Sodium citrate and glutathione were used as stabilizing agents while sodium sulfide was used as the sulfur source. The solution was heated at 95 °C for 1 h followed by in situ growth of the shell via the addition of zinc acetate and thiourea at 1:1 ratio to form CIS/ZnS core/shell QDs.

Synthesis of meso-5, 10, 15, 20-tetrakis (4-hydroxyphenyl) porphyrin

The synthesis was carried out according to Rojkiewicz et al.[19] method with modifications. Typically, an equimolar solution of 4-hydroxybenzaldehyde in propionic acid (1:1, v/v) was refluxed for 15 min at 45 °C. 1.42 mL of pyrrole was added quickly. The resulting mixture was refluxed for an additional 1.5 h followed by evaporation of the solvents and cooling. The residue was neutralized with $NaHCO_3$. The precipitated crude porphyrin was washed with chloroform and finally chromatographed on silica gel column using ethyl acetate: hexane (2:1, v/v) mixture.

Preparation of CIS/ZnS-mTHPP conjugate

The 3 mL of as-synthesized CIS/ZnS QDs was added to 1 mL of mTHPP. Conjugation of CIS/ZnS QDs with mTHPP was achieved via magnetic stirring.

Characterization

The synthesized CIS/ZnS QDs, mTHPP, and the conjugate were characterized using, Ultraviolet–visible spectrophotometry (UV–vis) (Perkin Elmer UV–Vis Lambda 25 spectrometer, UK), Photoluminescence (PL) (RF-6000, Shimadzu, Japan), Fourier Transform infrared spectroscopy (FTIR) (Spectrum two UATR spectrometer, Perkin Elmer, UK). Transmission electron microscopy (TEM) measurements were carried out using JEOL 2010 operated at 200 kV. x-ray diffraction (XRD) patterns of the as-synthesized QDs were collected by using PANalytical X'Pert x-ray diffractometer using a monochromatic Cu K_α radiation ($\lambda = 0.15406$ nm) at room temperature.

Singlet oxygen generation

Singlet oxygen generation was determined by the Adarsh et al.[20] method. Briefly, 1, 3-diphenylbenzofuran (DPBF) solution [0.1 mL, 0.2 mg/10 mL dimethyl sulfoxide (DMSO)] was diluted to 5.1 mL using DMSO. Then, 1:1 mixture of DPBF and mTHPP and 1:1 mixture of DPBF and conjugate were irradiated at 657 nm using spectro-fluorophotometry laser light for 365 s. The decrease in the intensity of DPBF was monitored at 471 nm. The singlet oxygen quantum yield (SOQY) was calculated against methylene blue as a standard (SOQY = 0.52) using the following formula:

$$\mathrm{SOQY} = \left(\frac{m_c}{m_{ref}}\right) \times \left(\frac{A_{ref}}{A_c}\right) \times \mathrm{SOQY}_{ref},$$

where SOQY and SOQY_{ref} are the singlet oxygen quantum yield of the sample (mTHPP or conjugate) and the reference (methylene blue, 0.52), m_c and m_{ref} are the slope of the sample and reference, A_{ref} and A_c are the absorbance of the reference and conjugate at irradiation wavelength.

Results and discussion

The optical properties of the as-synthesized CIS/ZnS QDs were recorded using UV–vis absorption and fluorescence spectroscopy. Figure 1(a) shows an emission spectrum of the as-synthesized CIS core with maximum PL emission at 538 nm. After passivation with ZnS shell, the PL maximum becomes red-shifted to 619 nm with increase in intensity. This increase is attributed to effective passivation of the surface defects causing non-radiative recombination after ZnS shell formation. Figure 1(a) "inset" shows the fluorescence image of the QDs solution with the UV lamp ($\lambda_{exc} = 352$ nm). The CIS QDs emit in the green region while the CIS/ZnS QDs emits in the orange region. Figure 1(b) shows the UV absorption spectra of the CIS core and core–shell with an absorption edge at higher energy compared with the bulk material. Similar spectrum had been reported for CIS core–shell QDs.[18]

The TEM micrographs of the CIS core and CIS/ZnS QDs core/shell in Figs. 2(a) and 2(b) show the presence of small, spherical, and mono-dispersed particles. The average particle size of the CIS core was estimated to be 3.0 ± 0.42 nm which increased to 3.5 ± 0.91 nm for the CIS/ZnS core/shell. The increase in particle size from the core to core/shell was attributed to the passivation of the core by the ZnS shell. XRD patterns of CIS/ZnS core/shell QDs [Fig. 2(c)] show three major peaks which closely lie to ZnS crystal phase (JCPDS 05-0566) compared with $CuInS_2$ crystal phase (JCPDS 27-0159). This is often reported in such core/shell materials where XRD patterns match the shell structures than that of the core.[18, 20] The broadness of the diffraction peaks of the

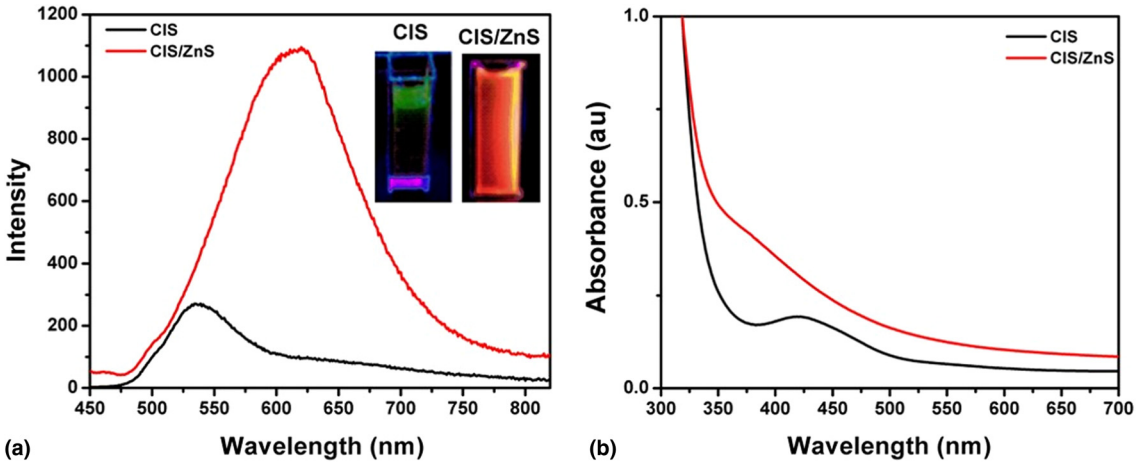

Figure 1. (a) PL Spectra of CIS core and CIS/ZnS core/shell QDs, *inset*: irradiation under UV light and (b) corresponding UV–vis absorption spectra.

XRD could be attributed to the nano-crystalline nature of core/shell QDs which is further confirmed by the corresponding ring patterns in selected area electron diffraction (SAED) pattern [Fig. 2(c), Inset].

Meso—5, 10, 15, 20-tetrakis (4-hydroxyphenyl) porphyrin (mTHPP) was obtained by condensation of 4-hydroxybenzaldehyde with pyrrole in acidic medium. UV absorption and ^{1}H NMR was used to ascertain successful synthesis of this heterocyclic compound. The synthesized mTHPP display characteristic absorption patterns (Fig. 3) with an intense Soret band at 418 nm and four weak Q-bands from 516 to 650 nm [Fig. 3(a) inset]. ^{1}H NMR spectra of mTHPP in DMSO as shown in Fig. S1 display chemical shifts at 9.97, 8.86, 7.98–8.00, 7.13–7.21, and −2.89 which are assigned to –OH, *β*-pyrrole, 2.6-phenyl, 3.5 phenyl, and N–H protons, respectively. The presence of the peak at −2.89 is assigned to the two inner protons of the pyrrole. This serves as confirmation that a free-base porphyrin was successfully synthesized.[21]

The photo-physical properties of the CIS/ZnS–mTHPP conjugate were investigated and the data were compared with that of the CIS/ZnS and mTHPP alone. Figure 3(b) shows that the conjugate preserves the spectroscopic characteristics of both CIS/ZnS QDs and mTHPP porphyrin. Notable is the presence of all four Q-bands of mTHPP with a little shift indicating the formation of conjugate [Fig. 3(b) inset]. Figure 3(c) shows the TEM image of the conjugate, which reveals that the size of the core/shell QDs increased after conjugation with mTHPP. The formation of conjugate is also significantly reflected in FTIR spectra where the hydroxyl and carbonyl bands of the QDs are shifted to higher wavenumbers after conjugation with mTHPP [Fig. 3(d)].

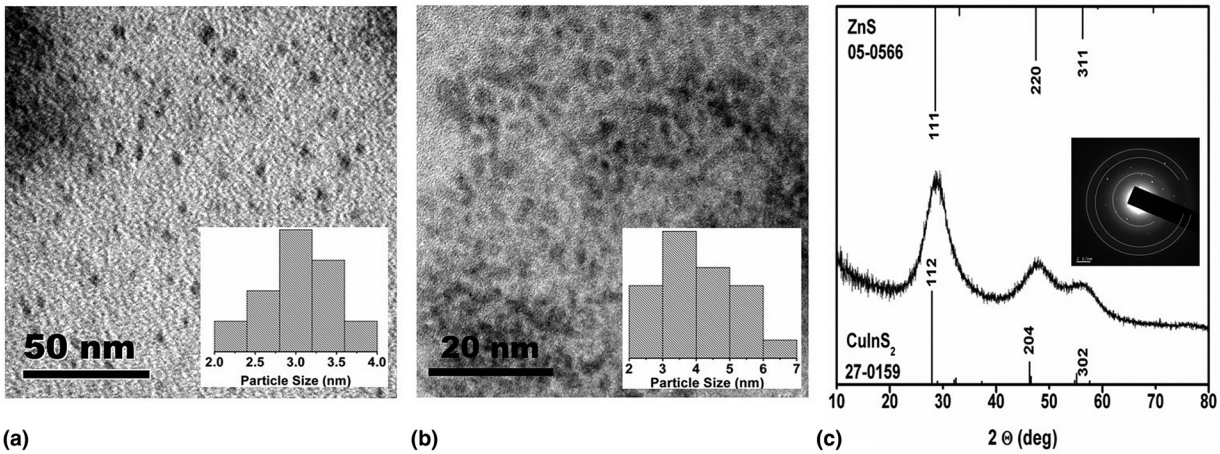

Figure 2. TEM micrographs of (a) CIS, (b) CIS/ZnS QDs, *inset*: corresponding particle size distribution graphs, and (c) XRD of CIS/ZnS QDs, *inset*: corresponding SAED pattern.

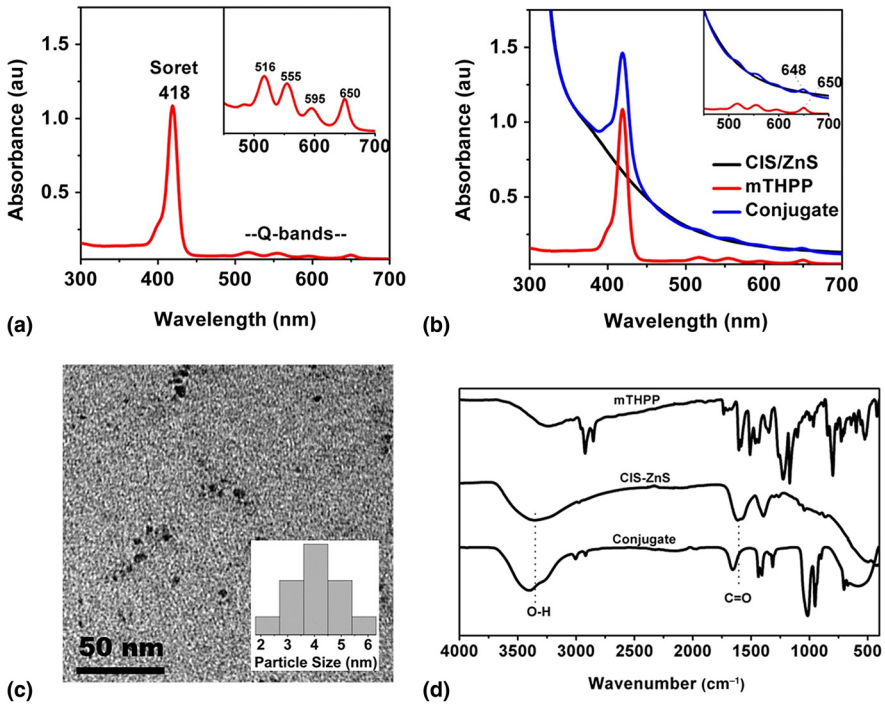

Figure 3. (a) UV–vis absorption spectra of mTHPP, *inset*: corresponding enlarged spectrum, (b) UV–vis absorption spectra of mTHPP, CIS/ZnS QDs and conjugate, *inset*: corresponding enlarged spectra, (c) TEM micrograph of mTHPP–CIS/ZnS QDs conjugate, Inset: corresponding particle size distribution graph, (d) FTIR spectra of mTHPP–CIS/ZnS QDs and the conjugate.

The generation of singlet oxygen forms the center of PDT mechanism. In this study, the singlet oxygen generation was achieved by monitoring the intensity of DPBP, singlet oxygen absorber, in both mTHPP [Fig. 4(a)] and the conjugate [Fig. 4(b)]. A decrease in DPBF intensity indicates oxidation of DPBF by singlet oxygen generated by the PSs. The SOQY was estimated to be 0.27 for mTHPP and 0.72 for the conjugate. This indicates that conjugation of CIS/ZnS to mTHPP enhanced the SOQY and improved the efficiency of mTHPP by almost three times as a PS for PDT application. Although

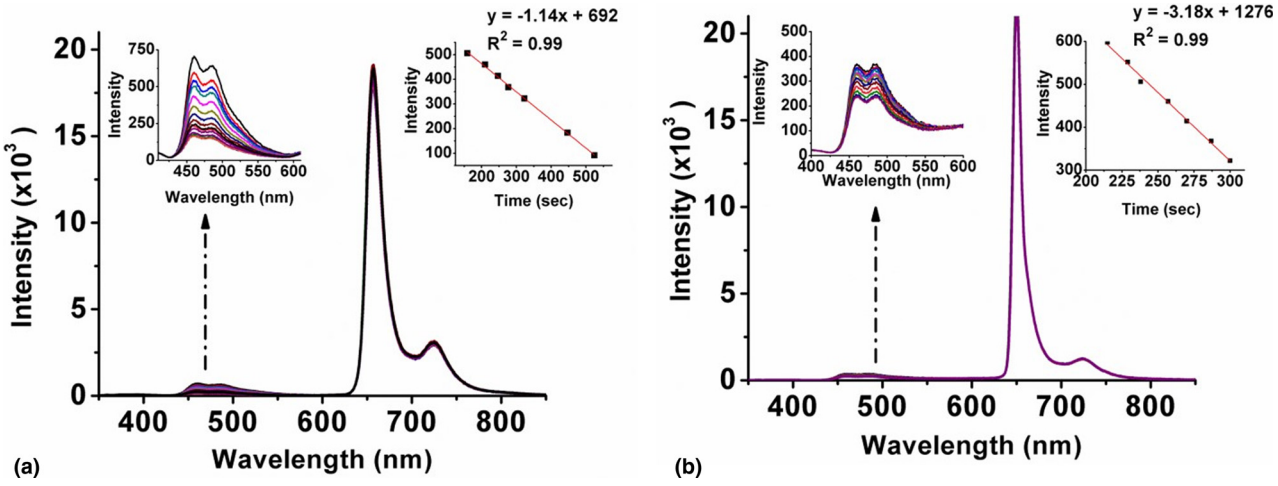

Figure 4. (a) Changes in the absorption spectrum of DPBF in presence of mTHPP and (b) in the presence of mTHPP–CIS/ZnS QD conjugates.

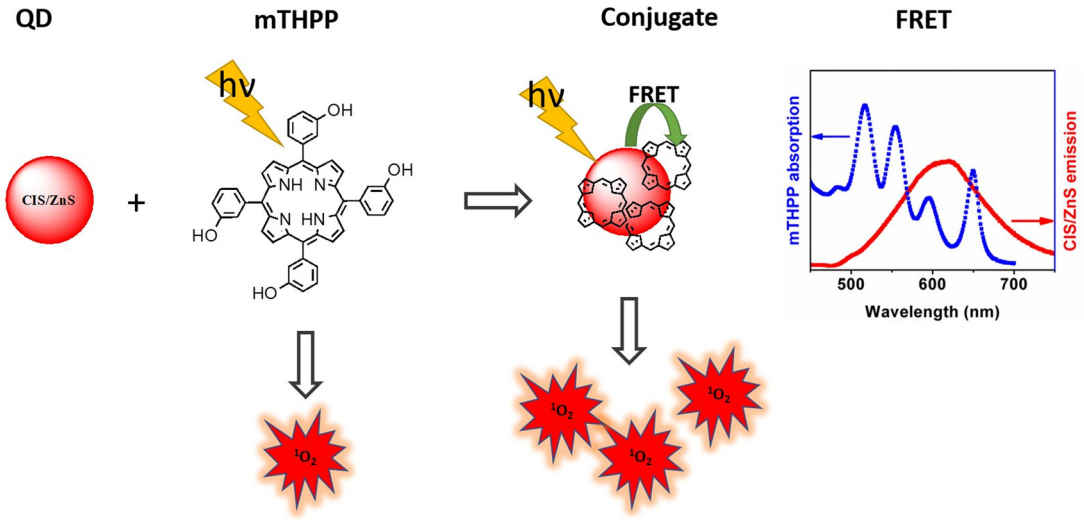

Scheme 1. Schematic diagram depicting improved singlet oxygen generation by mTHPP–CIS/QDs conjugates and their FRET spectral profile.

the study of fluorescence resonance energy transfer (FRET) is beyond the scope of this study, it is worth noting that, the spectral overlap and the close proximity of the mTHPP absorption and CuInS/ZnS fluorescence emission (Scheme 1) suggest a possible transfer in energy or electron between the QDs and porphyrin upon conjugation. It is also worth stating that mTHPP and mTHPP–CIS/ZnS conjugate did not exhibit any spectral changes when continuously irradiated with light at 657 nm in the absence of DPBF thus, indicating the photostability of the as-synthesized materials. Furthermore, the solubility of the conjugate was tested by drying the conjugate and re-dissolving it in water. This was repeated three times, and, in all instances, the conjugate was completely soluble in water (Fig. S2) and remained stable without any aggregation over 6 months.

Conclusions

In summary, we reported successful conjugation of ternary $CuInS_2$/ZnS QDs to meso-5, 10, 15, 20-tetrakis (4-hydroxyphenyl) porphyrin. The as-synthesized conjugate is highly water-soluble and stable for over 6 months. Quantitative analysis of the conjugate showed enhanced singlet oxygen generation compared with the mTHPP alone. The conjugate, therefore, proved to be efficient PS for photodynamic therapy application.

Supplementary material

The supplementary material for this article can be found at https://doi.org/10.1557/mrc.2018.60

Acknowledgments

The authors like to thank National Research Foundation (NRF), South Africa under the Competitive Programme for Rated Researchers (Grant no: 106060) and Thuthuka (Grant no: 107295) for financial support. The authors also acknowledge Cape-Peninsula University, under the Teaching Development Grant for the study leave granted to N. T.

References

1. R.R. Allison, and K. Moghissi: Photodynamic therapy (PDT): PDT mechanisms. *Clin. Endosc.* **46**, 24–29 (2013).
2. A.P. Subramanian, S.K. Jaganathan, A. Manikandan, K.N. Pandiaraj, N. Gomathi, and E. Supriyanto: Recent trends in nano-based drug delivery systems for efficient delivery of phytochemicals in chemotherapy. *RSC Adv.* **6**, 48294–48314 (2016).
3. T.A. Debele, S. Peng, and H.C. Tsai: Drug carrier for photodynamic cancer therapy. *Int. J. Mol. Sci.* **16**, 22094–22136 (2015).
4. B.W. Henderson, and T.J. Dougherty: How does photodynamic therapy work? *Photochem. Photobiol.* **55**,145–157 (1992).
5. N. Malatesti, I. Munitic, and I. Jurak: Porphyrin-based cationic amphiphilic photosensitisers as potential anticancer, antimicrobial and immunosuppressive agents. *Biophys. Rev.* **9**, 149–168 (2017).
6. H. Huang, W. Song, J. Rieffel, and J.F. Lovell: Emerging applications of porphyrins in photomedicine. *Font. Phys.* **3**, 1–15 (2015).
7. H. Abrahamse, and M. Hamblin: New photosensitizers for photodynamic therapy. *Biochem. J.* **473**, 347–364 (2016).
8. T.A. Debele, S. Peng, and H.C. Tsai: Drug carrier for photodynamic cancer therapy. *Int. J. Mol. Sci.* **16**, 22094–22136 (2015).
9. Z. Luksiene: Photodynamic therapy: mechanism of action and ways to improve the efficiency of treatment. *Medicina (B. Aires)* **39**, 1137–1149 (2003).
10. O.S. Viana, M.S. Ribeiro, A.C.D. Rodas, J.S. Rebouças, A. Fontes, and B.S. Santos: Comparative study on the efficiency of the photodynamic inactivation of Candida albicans using CdTe quantum dots, Zn(II) porphyrin and their conjugates as photosensitizers. *Molecules* **20**, 8893–8912 (2015).
11. D.O. Oluwole, and T. Nyokong: Physicochemical behavior of nanohybrids of mono and tetra substituted carboxyphenoxy phthalocyanine covalently linked to GSH-CdTe/CdS/ZnS quantum dots. *Polyhedron* **87**, 8–16 (2015).
12. M.F. Frasco, V. Vamvakaki, and N. Chaniotakis: Porphyrin decorated CdSe quantum dots for direct fluorescent sensing of metal ions. *Nanopart. Res.* **12**, 1449–1458 (2010).
13. R. Rotomskis and G. Streckyte: In *Quantum Dots in PDT, Imaging in Photodynamic Therapy*, edited by M.R. Hamblin, and Y. Huange (Taylor and Francis, London, New York, 2017), pp. 183–210.

14. S. Parani, G. Bupesh, E. Manikandan, K. Pandian, and O.S. Oluwafemi: Facile synthesis of mercaptosuccinic acid-capped CdTe/CdS/ZnS core/double shell quantum dots with improved cell viability on different cancer cells and normal cells. *J. Nanopart. Res.* **18**, 347 (2016).
15. X. Kang, Y. Yang, L. Huang, Y. Tao, L. Wang, and D. Pan: Large-scale synthesis of water-soluble $CuInSe_2$/ZnS and $AgInSe_2$/ZnS core/shell quantum dots. *Green Chem.* **17**, 4482–4488 (2015).
16. N. Tsolekile, S. Parani, M.C. Matoetoe, S.P. Songca, and O.S. Oluwafemi: Evolution of ternary I–III–VI QDs: synthesis, characterization and application. *Nano-Struct. Nano-Objects* **12**, 46–56 (2017).
17. C. Neela Mohan, V. Renuga, and A. Manikandan: Influence of silver precursor concentration on structural, optical and morphological properties of Cu1-xAgxInS2 semiconductor nanocrystals. *J. Alloys Compd.***729**, 407–417 (2017).
18. Y. Chen, S. Li, L. Huang, and D. Pan: Low-cost and gram-scale synthesis of water soluble Cu–In–S/ZnS core/shell quantum dots in an electric pressure cooker. *Nanoscale.* **6**, 1295–1298 (2014).
19. M. Rojkiewicz, P. Kuś, P. Kozub, and M. Kempa: The synthesis of new potential photosensitizers. *Dye Pigment* **99**, 627–635 (2013).
20. N. Adarsh, R.R. Avirah, and D. Ramaiah: Tuning photosensitized singlet oxygen generation efficiency of novel Aza-BODIPY dyes. *Org. Lett.* **12**, 5720–5723 (2010).
21. M.R. Dayer, A.A.M. Movahedi and M.S. Dayer: Band Assignment in Hemoglobin Porphyrin Ring Spectrum: Using Four-Orbital Model of Gouterman. *Protein Pept Lett* **17**, 473–479 (2010).